Determination of paracetamol in some headache medicines using modifier biosorbent

Elhossein A. Moawed[*,1]**, Heba O. El Sharawy**[1]**, Mohamed F. El-Shahat**[2]

Abstract— A novel biosorbent was synthesized by esterification of oleic acid with treated citrus sinensis using glacial acetic acid. The lignin citrus sinensis oleic sorbent (LCSOS) was characterized by ultraviolet/visible/infrared spectra, scanning electron microscope, conductivity, iodine/methylene blue number and Boehm titration. The electrical conductivity (σ) value for LCSOS was 1.9×10^{-9} $\Omega^{-1}cm^{-1}$. The acidic and basic sites were 13.4 and 2.4 mmol/g, it was clear that LCSOS had an acidic character. The LCSOS was success applied for spectrophotometric determination of paracetamol in pharmaceutical samples. The effecting of pH, contact shaking time, concentration, and solution temperature on the separation behavior of paracetamol onto LCSOS were studied. Also, the kinetics, equilibrium isotherms, and thermodynamic models for paracetamol separation from LCSOS were examined. Thermodynamic parameters such as enthalpy (ΔH), entropy (ΔS) and Gibbs free energy (ΔG) were (-37.4 kJ/mol, -112.4 J/mol. K and -3.86 kJ/mol) for paracetamol. The values of LOD and LOQ are 0.05 and 0.02 mg/mL, respectively for paracetamol.

Keywords: Biosorbent; Citrus sinensis; Paracetamol; Detection; Determination

1 INTRODUCTION

Paracetamol (acetaminophen, $C_8H_9NO_2$, 151.2 g/mol) is used as hypothermia, pain reliever in dental, back pain and headache cases. There are basic compounds that act as a natural chemical stimulant for the central nervous system [1-3]. The methods most frequently used for the determination of paracetamol in pharmaceutical samples were spectrophotometric methods [4-8]. This method was insensitive and selective, therefore the preconcentration and separation of paracetamol from its samples are appropriate for increasing of sensitive and selective of the spectrophotometer methods.

Among different separation techniques solid phase extraction (SPE) based on adsorption, ion-exchange or chelating properties of solid sorbents was found to be the most effective [9-12]. More recently, biosorbent has attracted scientific interest as they exhibit excellent and unique physical properties such as high surface area, low density, good thermal and electrical conductivity [13, 14]. Numerous methods have been developed to improve the biosorbent to increase the quantity of surface functional groups [15-17]. Chemical oxidation, acidic/alkaline or salt modified with H_2O_2, HNO_3, HCl, NaOH or $ZnCl_2$ has been widely applied for the development of biosorbent for extraction of organic species [18-20].

Orange tree (Citrus sinensis, CS) is one of the most famous citruses which a good source of alkali and vitamins A and C. Mediterranean countries are best areas for the growth of orange trees [21, 22]. The main chemical composition of orange trees is water, fats, proteins, minerals, and carbohydrates. Citrus sinensis consists of cellulose; hemicellulose, lignin, and fibers. Lignin may be defined as a very irregular, randomly cross-linked polymer of phenylpropane units joined by many different linkages and an amorphous. Lignin can be hydrolyzed and extracted from wood or converted to a soluble derivative.

In the present work, a new biosorbent (lignin citrus sinensis oleic sorbent, LCSOS) was prepared by coupling of citrus sinensis with oleic acid. This type eliminates the problem of low stability of normal biosorbent. The interfacial bond between the oleic acid and the citrus matrix can be enhanced by enlarging the surface area, which provides more sites of contact/anchorage and interactions between the biosorbent and the analytes. The characterization of the LCSOS showed that it has high capacity and stability, which has been recycled many times after regeneration using NH_4OH (1:1), HCl (1:1) and H_2O without decreasing their capacities. Also, the LCSOS was found to be very stable toward the acids, alkalis and organic solvents. The sorption behavior of paracetamol onto LCSOS has been studied to optimize the best conditions for separation and preconcentration of paracetamol from aqueous solution. Data have been obtained for kinetic, thermodynamic, and equilibrium situations. The proposed method had been successfully applied for extraction of paracetamol from different samples of pharmaceutical.

2-Experimental

2.1. Materials and reagents

A 100 mL of 5 mg/mL stock solutions of paracetamol (El-Nasr, Cairo, Egypt) was prepared. A series of 25 mL of standard solutions (0.01-0.1 mg/mL) were used for the calibration curves. To prepare lignin citrus sinensis (LCS): A 100 g of citrus sinensis washed with distilled water followed by methanol, and dried at 100 ºC. Citrus sinensis was soaked in glacial acetic acid stirred for three hours and washed with distilled water and dried at 100 ºC. To prepare the lignin citrus sinensis oleic sorbent (LCSOS): 5 g of the preparation lignin citrus sinensis (LCS) were coupled with 25 mL oleic acid and 25 mL toluene then refluxed for three hours, and dried at 60 ºC.

2.2. Apparatus

All spectrophotometric measurements were performed on a JASCO (V-630 UV-VIS Spectrophotometer, Japan). Scanning electron microscope analysis was carried out using JEOL model JSM-6510LV apparatus, manufactured in the USA. IR spectra were carried out using KBr disc on a JASCO FTIR-410 spec-

trometer in the 4000–400 cm^{-1} regions. Bulk DC conductivity was measured using 6517B electrometer-high resistance meter after pressing CS, LCS, and LCSOS disk by a Hydraulic press at 10 tons in the form of a circular disk and potential equal to 1 volt.

2.3. Recommended procedures

A 25 mL of paracetamol solutions were shacked with 0.1 g of LCSOS at desired pH and times. After 30 minutes, the sample solutions were filtered then the remained and recovered concentrations were measurement spectrophotometrically.

3. Results and discussion

3.1. Characteristics of citrus sinensis

The infrared spectrum of CS, LCS, and LCSOS were tested using KBr disc in the range of 4000–400 cm^{-1} (Fig. 1). The spectrum of CS showed the presence of the following groups: OH/NH$_2$ (3753-2978 cm^{-1}), CH aromatic (2922 cm^{-1}), CH aliphatic (2852 cm^{-1}), C=O (1736 cm^{-1}), C=C (1630 cm^{-1}), C–O (1471 cm^{-1}), and C-O-C, CH or COOR (1240, 1045 cm^{-1}). The bands of LCS spectrum were shifted to 3373, 2937, 2895, 1724, 1632, 1470, 1240, 1031 cm^{-1} due to presence OH, CH aromatic and aliphatic, C=O, C=C, C–O, and C-O-C, CH or COOR groups due to formation of lignin after coupling with glacial acetic acid. In the LCSOS spectrum, peaks for CH aromatic, CH aliphatic, C=O, and C-O were developed at 2926, 2854, 1709 cm^{-1} and 1433 cm^{-1}. The band of υ OH, C=C, and C-O-C, CH or COOR groups were disappeared due to esterification with oleic acid.

UV-VIS electronic spectra of CS, LCS, and LCSOS were recorded in the solid state using Nujol mulls method in the range of 200 to 400 nm (Fig. 2). Higher energy spectra bands of CS were assigned to 236-269, 271, and 281 nm were attributed to π–π* transitions and bands at 285-353, 357, and 369-370 nm were attributed to n–π* transitions. LCS spectrum has many bands at 236-269, 271, and 281 nm which attributed to π–π* transitions, and the bands were developed to 285-346, and 370 nm due to formation of lignin after coupling with glacial acetic acid which attributed to the n- π* transitions. The higher energy spectra of LCSOS were attributed to 237-269, 271, 281 dues to the π–π* transitions, band at 285-370 nm were shifted due to esterification with oleic acid which attributed to the n- π* transitions localized on the conjugated system.

Acidic and basic sites of CS, LCS, and LCSOS were estimated by Boehm titrations (Table 1). Basic and acidic groups were determined by back titration of the filtrate with standard HCl and NaOH solution (0.1 mol/L). CS has 3.2 mmol/g of phenolic group, 6.1 mmol/g of carbonyl group and 6.3 mmol/g carboxyl group. It clears that the amount of lactonic and phenolic sites was decreased in LCS to 4.3 mmol/g after coupling with glacial acetic acid, unlike the amount of lactonic and phenolic sites was increased in LCSOS to 9.6 mmol/g when compared with CS (9.3 mmol/g) due to esterification with oleic acid. The estimated acidic and basic sites were 15.6 and 1.8 mmol/g for CS, 5.9 and 2.1 for LCS, and 13.4 and 2.4 for LCSOS. By com-

paring the acidic sites and the basic ones of CS, LCS, and LCSOS, it is clear that the total acidic sites were greater than total basic sites that they have mainly acidic character.

The pH$_{ZCP}$ (zero charge point) is the pH which the charge of surface is zero. The pH$_{ZCP}$ of CS, LCS, and LCSOS were 6.6, 5.01 and 3.1, respectively. Maximum values of ΔpH was 0.88, -3.17 at pH=5.02, 9.12 for CS, 0.5, -4.04 at pH=3.06, 9.12 for LCS, and -4.67 at pH=9.12 for LCSOS (Fig. 3). Based on the pH$_{ZCP}$ values, LCSOS is more acidic than the CS and LCS. The surface of CS, LCS and LCSOS is positively charged at pH lower than 6.6, 5.01 and 3.1 due to the protonation of the surface functional groups in acidic medium while the surface is negatively charged above pH 6.6, 5.01 and 3.1 due to deprotonation of the surface.

The densities of CS, LCS, and LCSOS were estimated. The densities of CS, LCS, and LCSOS were 0.48, 0.30 and 0.68 g/cm^3. The results obtained clear that LCS decreased after coupling with glacial acetic acid. The density of LCSOS is higher than LCS due to esterification with oleic acid.

The values of electrical conductivity (σ) for CS, LCS, and LCSOS were measured in the solid state which found to be 2.6x10^{-9} Ω^{-1} cm^{-1}, 1.3x10^{-9} Ω^{-1} cm^{-1}, and 1.9x10^{-9} Ω^{-1} cm^{-1}, respectively. The results were shown that the value of conductivity of LCSOS is higher than LCS due to coupling with oleic acid, and conductivity of LCS lower than CS after coupling with glacial acetic acid.

The iodine number (I$_2$ No) is a technique used to determine the adsorption capacity and defined as the internal surface of an adsorbent and detecting microspores (0-2 nm). The Iodine number of prepared CS, LCS, and LCSOS were measured by back titration of I$_2$ with Na$_2$S$_2$O$_3$ (0.05 mol/L) based on the standard method. The values of iodine number (I$_2$ No) for CS, LCS, and LCSOS were 1.93, 1.75 and 2.45 mmol/g (244.3, 222.1 and 310.9 mg/g). These indicate that the I$_2$ No value of LCSOS is higher than LCS due to coupling with oleic acid, and I$_2$ No of LCS decreased from CS by addition glacial acetic acid. Methylene blue value (MB value) is a widely used technique to determine the cation-exchange capacity and mesoporous (2-50 nm). Methylene blue value (MB) for CS, LCS, and LCSOS were 2.91, 2.85 and 2.97 mmol/g (931, 912 and 950 mg/g), respectively. The MB for LCSOS was higher than the MB of CS and LCS. The obtained results indicated that the I$_2$ No depends on the adsorption process while the MB value depends on the cation-exchange process.

A scanning electron microscope (SEM) is a type of electron microscope that produces images of a sample by scanning the surface with a focused beam of electrons. The electrons interact with atoms in the sample, producing various signals that contain information about the sample's surface topography and composition. An electron microscope that moves a narrowly focused beam of electrons across an object and detects the patterns made by the electrons scattered by the object and the electrons knocked loose from the object. From these patterns a three-dimensional image of the object is created. The morphology of LCSOS composite was investigated using JEOL model JSM-6510LV analytical scanning electron microscopy at magnifications from 150x to 2000x. (Fig 4), represent SEM images of the lignin citrus sinensis oleic sorbent (LCSOS) at magnifications of 150, 250, 500, 750, 1000, and 2000.

The microstructure of LCSOS images showed that the surface is relatively smooth. And the cells are irregular in size and distribution. The surface of LCSOS contains holes, channels, and caves. It contains many pores with different pore size ranged nano scale to micro scale, indicated that the LCSOS has a good characteristic to be employed as a sorbent.
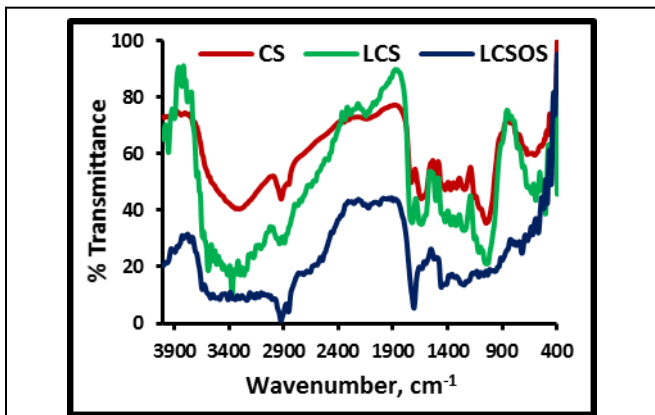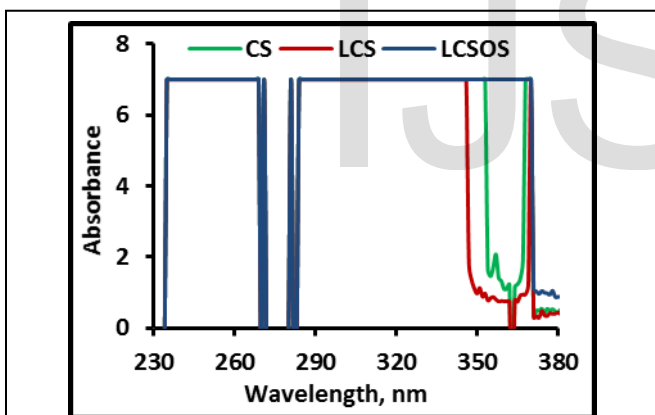

Fig. 1. The infrared spectra of CS, LCS, and LCSOS

Fig 2. UV-Vis spectra of CS, LCS, and LCSOS

Table 1
Boehm titration of CS, LCS and LCSOS

Material	Acidic sites mmol/g	Basic sites mmol/g
CS	3.2	1.8
LCS	1.2	2.1
LCSOS	3.5	2.4

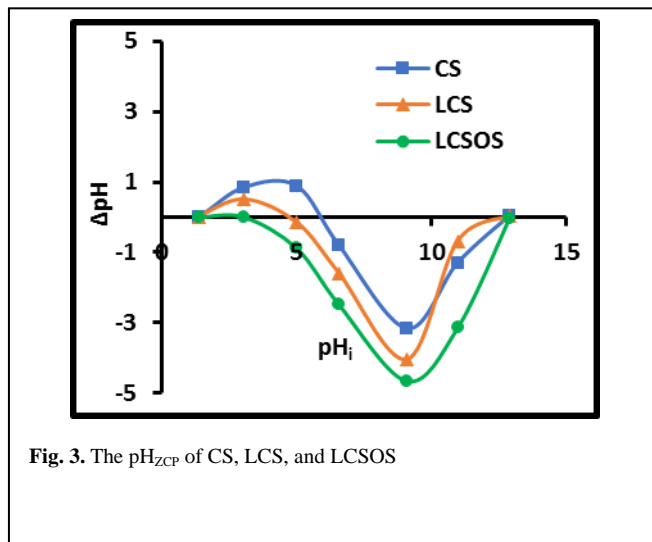**Fig. 3.** The pH_{ZCP} of CS, LCS, and LCSOS

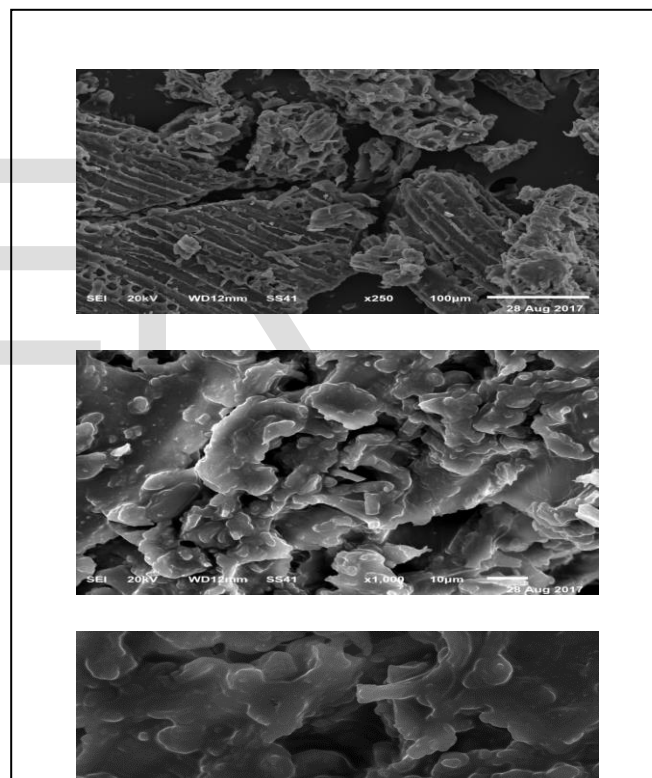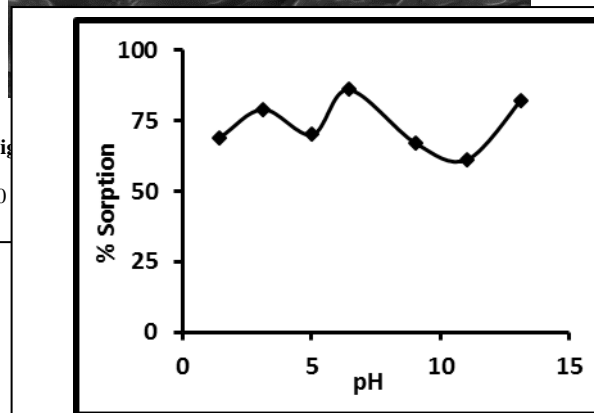**3.2. Optimum**

Fig. 5. Effect of the sample pH on the sorption of paracetamol using LCSOS

conditions for separation of paracetamol using LCSOS

3.2.1. Effect of sample pH

The effect of the sample pH on the sorption behavior of para-cetamol was studied in the pH range of 1-13 using 25 ml of a sample solution. The sample were processed according to the recommended batch experiments. The pH_{ZCP} value of LCSOS was determined to be 3.1. Fig. 5 was shown that the maximum sorption percentages were achieved at pH range 3.1 and 6.43 for paracetamol (79%, and 86%). It is clear that the electrostatic attraction between anionic drug (paracetamol) and the posi-tively charged functional groups on the surface of LCSOS would take place at pH 3.1. On the contrary, an increase in the medium pH value hinders sorption because of increasing the negative charge on LCSOS surface which results in electrostat-ic repulsion between paracetamol and LCSOS.

3.2.2. Effect of contact time

Effect of contact time (5-30 min) of paracetamol was carried out. The time required for maximum sorption of paracetamol onto LCSOS is 30 min (Fig 6). The sorption rate of the parace-tamol onto LCSOS is very rapid; it was accomplished (85-100%). This result indicates that the sorption rates and per-centages are depended on the nature of the reaction between paracetamol and the sorbent (LCSOS).

3.2.3. Effect of initial concentration

Fig. 7 was shown the effect of concentrations (0.06-0.66 mmol/L) or (0.01-0.1 mg/mL) for paracetamol on batch capaci-ty (Q_B) of LCSOS. The R^2 values of paracetamol was 0.9974, while those of the intercept was -0.0023. It was noticed that the increase of paracetamol concentrations is followed by a subse-quent increase in the sorption capacity of LCSOS. The value of Q_B for paracetamol onto LCSOS was calculated to be 0.15 mmol/g (22.7 mg/g). It is evident from this result the LCSOS has greater sorption capacity toward paracetamol than other sorbents (Table 2).

3.2.4. Effect of temperature

Fig. 8 was shown that the effect of solution temperature of parace-tamol (25–75 ℃) on the sorption percentages (10–95.8%). The sorp-tion percentages of paracetamol were slightly decreasing with in-creasing of temperature, the maximum sorption of paracetamol (95.8%) was observed at low temperature (25 ℃). Decreasing of sorption percentage at 40 ℃ is due to deformation of bonds between the paracetamol molecules and the active site of LCSOS. Then in-creasing in temperature to reach maximum sorption (80.3%) at 65 ℃ and then slightly decreasing to reach 72 ℃ at 70.1%.

Table 2

Sorption capacities of various sorbents for paracetamol

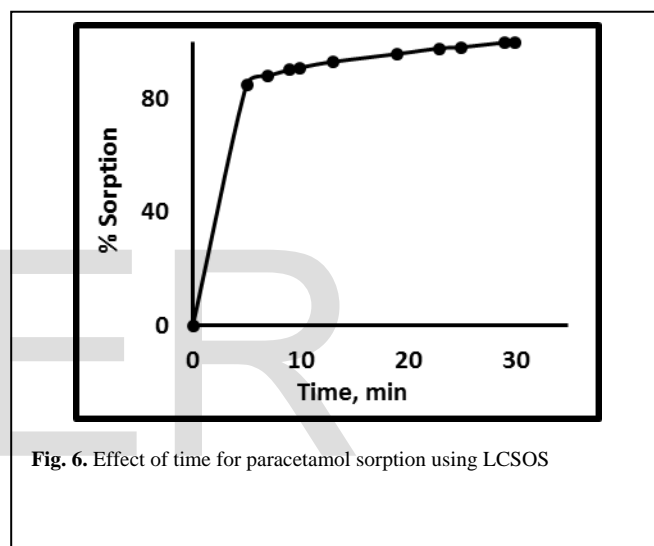| Sorbent	Q (mg/g)	References
Grape stake	1.74	[23]
Cork bark	0.99	[24]
Yohimbe bark	0.77	[24]
Dehydrated sewage sludge	0.96	[25]
Posidonia oceanica	1.64	[25]
LCSOS	22.7	This work

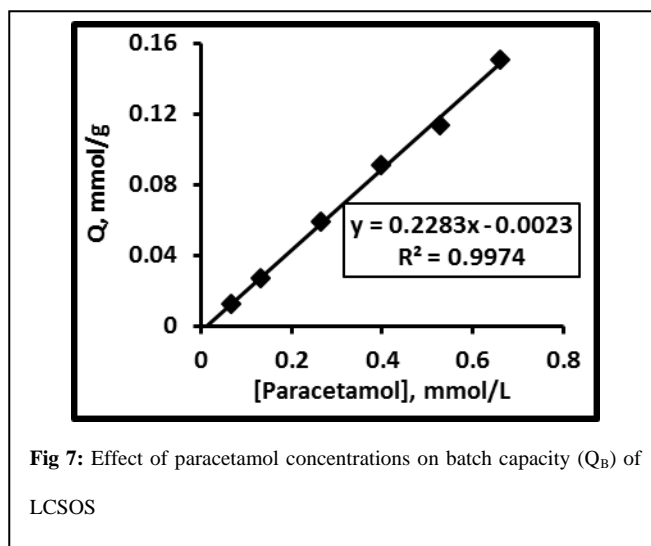**Fig. 6.** Effect of time for paracetamol sorption using LCSOS

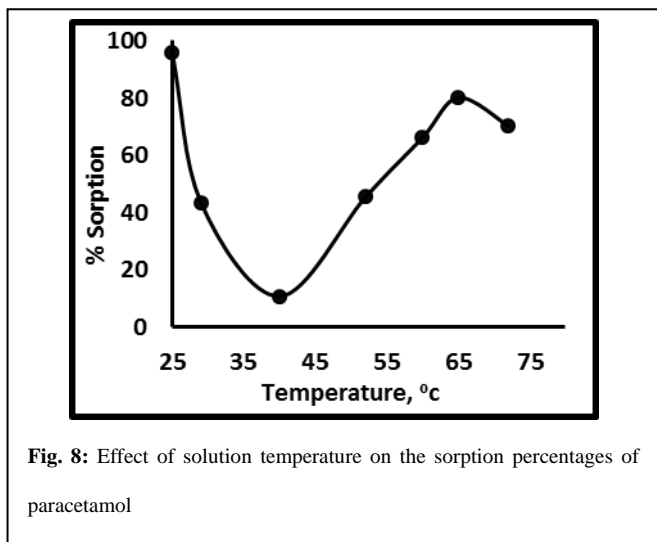**Fig 7:** Effect of paracetamol concentrations on batch capacity (Q_B) of

LCSOS

Fig. 8: Effect of solution temperature on the sorption percentages of paracetamol

3.3. Kinetic studies

Table 3 was shown that the kinetic parameters study for the sorption of paracetamol onto LCSOS by pseudo first order and pseudo-second-order. By comparing the correlation coefficient (R^2) values, the R^2 values of paracetamol suggest that pseudo-second-order sorption model (0.997) is predominant than pseudo-first-order (0.8609). Parameters of the kinetic pseudo-first-order model for sorption of drug were calculated. The rate constant of the sorption (k_1) values were 0.145 min^{-1}, the half-life time ($t_{1/2} = 0.693/k_1$) values was 4.78 min, and the capacity (Q_e) value were 0.039 mmol/g for paracetamol. Also, parameters of the kinetic pseudo-second-order model for sorption of drug were calculated. These parameters were k_2: 7.2 g/mmol. min, $t^{1/2}$: 1.35 min, and Q_e: 0.103 mmol/g for paracetamol.

3.4. Equilibrium studies

The equilibrium data estimated from the sorption isotherms are required to understand the sorption mechanism. The experimental data were analyzed using models such as Freundlich and Langmuir which were used to predict the adsorption capacities (Table 4). Based on R^2 from the comparison between Freundlich model (0.8317) and Langmuir model (0.2178) for paracetamol, it clears that Freundlich model is a good fit to interpreting the adsorption process with multilayer sorption on the heterogeneous surface of LCSOS.

3.5. Thermodynamic studies

Thermodynamic sorption behavior of paracetamol onto LCSOS was evaluated by thermodynamic parameters. The value of R^2 was 0.2114 for paracetamol sorption. The negative sign of Gibbs free energy change (ΔG) were -3.86 kJ/mol (Table 5) indicated the spontaneous nature of the sorption process. The negative ΔH value which revealed to the exothermic nature of the chemisorption process. The negative sign of ΔS was which indicates that the decrease in disorder at the solid/solution interface during the sorption process.

4. Accuracy and precision

Limit of detection (LOD) is the lowest concentration of the analyte that gives the measurable response. Limit of quantification (LOQ) is the lowest concentration of the analyte, which gives response that can be accurately quantified [26]. LOD and LOQ were calculated using the following equations: LOD=3σ/m and LOQ=10 σ/m. Where σ is the standard deviation of six replicate measurements of the low concentration of paracetamol and m is the slope of the calibration curve (Fig 9). The values of LOD and LOQ are 0.05 and 0.02 mg/mL, respectively. The result obtained show that the developed LCSOS sorption method offers higher sensitivity for determination of paracetamol when compared with other methods. The relative standard deviation (RSD%) and recovery percentage for the analysis of the studied paracetamol are 2.8 and 81%, respectively. The low value of RSD indicates a good precision and accuracy of the proposed method.

Table 3
Kinetic parameters of pseudo first order and pseudo second order models

Pseudo first order			Pseudo second order		
R^2	k_1	$t_{1/2}$	R^2	k_2	$t_{1/2}$
0.8609	0.145	4.78	0.997	7.2	1.35

Table 4
Comparison between Freundlich and Langmuir isotherm parameters

Table 5
Thermodynamic parameters for sorption of paracetamol

Langmuir isotherm			Freundlich isotherm		
R^2	K_L	b	R^2	K_F	n	1/n
0.2178	0.14	7.8	0.8317	8.2	1.36	0.71

ΔG	ΔH	ΔS
(kJ/mol)	(kJ/mol)	(J/mol. K)
- 3.86	-37.4	-112.4

5. Conclusions

Citrus sinensis (CS) was coupled with glacial acetic acid then was esterificated of oleic acid to prepare a new sorbent lignin citrus sinensis oleic sorbent (LCSOS) with acidic character. LCSOS was applied for the determination of basic medicine (paracetamol). The physicochemical characteristics of LCSOS were estimated. The effect of different factors including pH, solution temperature, initial concentration, and contact shaking time were evaluated. Kinetic and equilibrium studies was shown that Freundlich adsorption isotherm model and pseudo first order was fitted very well for the experimental results. It was clear the sorption process was exothermic and spontaneous in nature and has entropy at the solid-liquid interface of paracetamol with LCSOS disorder and ran-
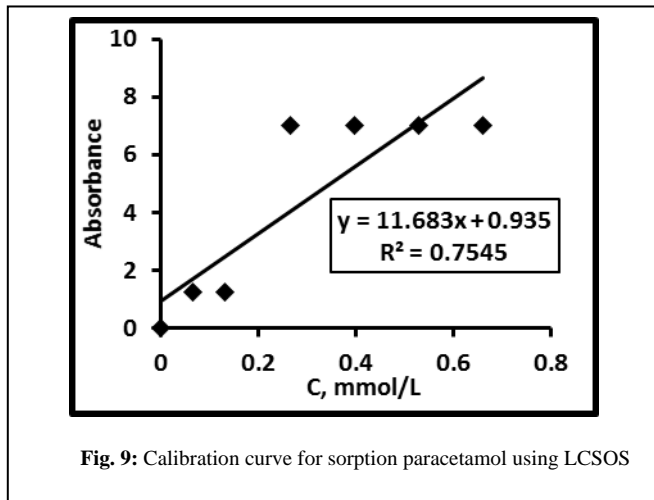
Fig. 9: Calibration curve for sorption paracetamol using LCSOS

domness decreased.

References

[1] S. A. Khaled, M. R. Alexander, R. D. Wildman, M. J. Wallace, S. Sharpe, J. Yoo , C. J. Roberts, 3D extrusion printing of high drug loading immediate release paracetamol tablets, International Journal of Pharmaceutics, 538 (2018) 223-230

[2] J. Rubbens, R. Mols, J. Brouwers, P. Augustijns, Exploring gastric drug absorption in fasted and fed state rats, International Journal of Pharmaceutics, 548 (2018) 636-641

[3] I. B. Rietveld, M. Barrio, P. Lloveras, R. Céolin, J. L. Tamarit, Polymorphism of spironolactone: An unprecedented case of monotropy turning to enantiotropy with a huge difference in the melting temperatures, International Journal of Pharmaceutics, 552 (2018) 193-205

[4] C. Xu, B. Li, Spectrophotometric determination of paracetamol with microwave assisted alkaline hydrolysis, Spectrochimica Acta Part A: Molecular and Biomolecular Spectroscopy, 60 (2004) 1861-1864

[5] M. R. Khoshayand, H. Abdollahi, M. Shariatpanahi, A. Saadatfard, A. Mohammadi, Simultaneous spectrophotometric determination of paracetamol, ibuprofen and caffeine in pharmaceuticals by chemometric methods, Spectrochimica Acta Part A: Molecular and Biomolecular Spectroscopy, 70 (2008) 491-499

[6] H. E. Abdellatef, M. M. Ayad, S. M. Soliman and N F Youssef, Spectrophotometric and spectrodensitometric determination of paracetamol and drotaverine HCl in combination, Spectrochimica Acta Part A: Molecular and Biomolecular Spectroscopy, 66 (2007) 1147-1151

[7] A. Ashour, M. A. Hegazy, M. Abdel-Kawy, M. B. ElZeiny, Simultaneous Spectrophotometric determination of overlapping spectra of paracetamol and caffeine in laboratory prepared mixtures and pharmaceutical preparations using continuous wavelet and derivative transform, Journal of Saudi Chemical Society, 19 (2015) 186-192

[8] S. Glavanović, M. Glavanović, V. Tomišić, Simultaneous quantitative determination of paracetamol and tramadol in tablet formulation using UV spectrophotometry and chemometric methods, Spectrochimica Acta Part A: Molecular and Biomolecular Spectroscopy, 157 (2016) 258-264

[9] S. Abbasi, S. A. Haeri, S. Sajjadifar, Bio-dispersive liquid liquid microextraction based on nano rhamnolipid aggregates combined with molecularly imprinted-solid phase extraction for selective determination of paracetamol in human urine samples followed by HPLC, Microchemical Journal, 146 (2019) 106-114

[10] H. İ. Ulusoy, E. Yılmaz, M. Soylak, Magnetic solid phase extraction of trace paracetamol and caffeine in synthetic urine and wastewater samples by a using core shell hybrid material consisting of graphene oxide/multiwalled carbon nanotube/Fe_3O_4/SiO_2, Microchemical Journal, 145 (2019) 843-851

[11] S. A. E. A. Mohamed, F. F. Belal, A micellar HPLC method for simultaneous determination of methocarbamol in three different tablets using single run; application to human plasma and evaluation of the method greenness, Microchemical Journal, 148 (2019) 262-269

[12] M. Massoudinejad, H. Rasoulzadeh, M. Ghaderpoori, Magnetic chitosan nanocomposite: Fabrication, properties, and optimization for adsorptive removal of crystal violet from aqueous solutions, Carbohydrate Polymers, 206 (2019) 844-853

[13] E. A. Moawed, M. A. El-Hagrasy, A. E. A. Senan, Application of bio-alkyd resin for the removal of crystal violet and methylene blue dyes from wastewater, International Journal of Environmental Science and Technology, (2019) https://doi.org/10.1007/s13762-019-02343-1

[14] E. A. Moawed, M. A. El-ghamry, M. A. El-Hagrasy, M. F. El-Shahat, Determination of iron, cobalt and nickel ions from aqueous media using the alkali modified miswak, Journal of the Association of Arab Universities for Basic and Applied Sciences, 23 (2017) 43-51

[15] A. C. Khorasani, S. A. Shojaosadati, Magnetic pectin-Chlorella vulgaris biosorbent for the adsorption of dyes, Journal of Environmental Chemical Engineering, 7 (2019) 103062

[16] E. A. Moawed, Effect of heating processes on Salvadora persica (Miswak) and its application for removal and determination of aniline blue from wastewater, Journal of Taibah University for Science, 7 (2013) 26–34

[17] E. A. Moawed and A B Abulkibash, Selective separation of Light green and Safranin O from aqueous solution using Salvadora persica (Miswak) powder as a new biosorbent, Journal of Saudi Chemical Society, 20 (2016) S178–S185

[18] E. A. Moawed, H. A. Kiwaan, A. A. A. Elbaraay, Synthesis and characterization of novel friendly biosorbents and it uses for removal of crystal violet dye from wastewater, International Journal of Scientific & Engineering Research, 10 (2019) 1259-1278

[19] E. A. Moawed; H A Kiwaan and M M Elshazly, Application of polyurethane@salvadora persica composite for detection and removal of acidic and basic dyes from wastewater, Journal of the Taiwan Institute of Chemical Engineers, 80 (2017) 894–900

[20] E. A. Moawed, A. E. Wahba, R. A. Gabr, Synthesis and application of LGB/St/Al_2O_3 biocomposite for sensitive detection and efficient removal of brilliant green dye from wastewater, Journal of Environmental Chemical Engineering, 6 (2018) 7225–7232

[21] K. A. Khalid, A. E. El-Gohary, A. M. A. Ahmed, F. M. A. M. Elkady, I. M. Talaat, L-tryptophan affects the essential oil of navel orange under various growing regions, Biocatalysis and Agricultural Biotechnology, 20 (2019)

[22] P. J. Barroso, J. Martín, J. L. Santos, I. Aparicio, E. Alonso, Evaluation of the airborne pollution by emerging contaminants using bitter orange (Citrus aurantium) tree leaves as biosamplers, Science of The Total Environment, 677 (2019) 484-492